A Method for Measuring Charge Separation in Granular Mixtures in Vacuum

Dylan Carter and Christine Hartzell
Dept. of Aerospace Engineering
University of Maryland at College Park
phone: (1) 301-538-8923
e-mail: d.p.carter4@gmail.com

Abstract - **Triboelectric charge exchange is a significant source of charge transfer in many granular phenomena, including dust storms, powder transport, and extraterrestrial environments. We previous developed a model to better predict the effects of tribocharging on the charge distribution of mixtures composed of a single material. We have designed an experiment to test these predictions. In our experiment, grains are baked to remove adsorbed water and are mixed in vacuum to induce tribocharging. The charged grains are dropped through an electric field, where high-speed imaging of the grains identifies their physical size and charge via their response to the field. This allows us to estimate the distribution of charge among grain sizes in the mixture, and the effect of pre-treatment conditions like temperature, pressure, and relative humidity. The data collected from this experiment will enable more accurate predictions to be made about the charging process in a variety of environments, especially the dusty, airless surface of asteroids and the Moon, where much remains unknown about charge transfer processes.**

I. Introduction

Triboelectric charging is responsible for the generation of large potential differences in a variety of granular media. In terrestrial environments, collisions between grains in sand storms [1-3] and ash clouds [4-5] generate electric fields sometimes strong enough to affect the dynamics of the cloud. In extraterrestrial environments like the Moon, Mars, and other bodies [6-11], tribocharging is known to occur, and dynamics in the surface regolith are often dominated by interparticle forces rather than gravitational forces. In environments like industrial pneumatic powder transport systems [12-14], granular media often experiences clumping and even electrical discharge due to charge separation. Despite great scientific interest in understanding the underlying mechanism of grain charging, there are few experiments that can make measurements of individual grain charges, largely rising from the difficulty in obtaining such precise measurements. Many experiments fall into one of two camps: some separate positive grains from negative, reducing the charge distribution to a simple binary polarity measurement [6-7, 15-16], while others measure the absolute charge of a bulk sample [17-20], which obscures the particle charge distribution from measurement. We previously developed a predictive model for the grain

charge distribution in continuous polydisperse mixtures of dielectric grains [21], but verification of the model requires a measurement technique that can resolve charge and size of individual grains.

We have developed a technique like that of Dr. Heinrich Jaeger and his group [22-23] for directly measuring the accumulated charge on individual grains, rather than simply measuring polarity or average charges. In this technique, grains are mixed in vacuum to induce triboelectric charge exchange, then dropped through a transverse electric field. We measure the acceleration of individual grains under the influence of this electrostatic force using high-speed videography, and extract charge and mass data from the observed acceleration and grain size, respectively. One notable change from the methodology of Jaeger, *et al*, is that we house the entire apparatus in high vacuum during operation, including during the mixing process. This allows significantly more control over the ambient conditions under which charging occurs. Specifically, by varying the amount of time the sample is exposed to vacuum prior to charging, we will be able to evaluate the effect of adsorbed water on the charging process.

II. EXPERIMENTAL SETUP

A schematic of our experimental setup is shown in Fig. 1. The entire mechanism is housed in a 30 in. tall, 24 in. wide, 24 in. deep vacuum chamber (not shown). The chamber is held at a constant pressure of 10^{-6} Torr. On one side of the device, a high-speed camera (PCO Dimax CS3, 4000 frames per second) is affixed to an aluminum carriage that rides along a low-friction self-lubricating rail, which is held at the top of the device by an electromagnet. On the other side, a small steel container filled with dielectric granular material (e.g., spherical SiO_2 beads, with average diameter d_{avg}) is vigorously shaken vertically at 28 Hz by a speaker. The interior of the container is coated in a thin layer of the same grains, preventing physical and electrical contact between the loose grains and the container walls. Furthermore, the grains are pretreated prior to mixing by baking them in a separate chamber to remove any water adsorbed on their surface. Mixing the grains in an insulated container and under high vacuum conditions induces triboelectric charge exchange between the grains in isolation of certain common external factors (adsorbed humidity [14, 24-27], atmospheric effects [28], and contact charging with the container [22]). This ensures that the grains carry a charge distribution consistent with models considering grain-to-grain charging only.

The grain mixing mechanism is suspended above a pair of parallel copper electrodes 15.75 in. tall and 4.25 in. wide. The electrodes carry a large potential difference V between them (variable, between 1000 V and 5000 V) and are spaced a distance $L = 5.87$ cm apart, such that there exists an electric field of strength $E = V/L$ in this region, directed from one plate to the other. Below this region is a large collection bin.
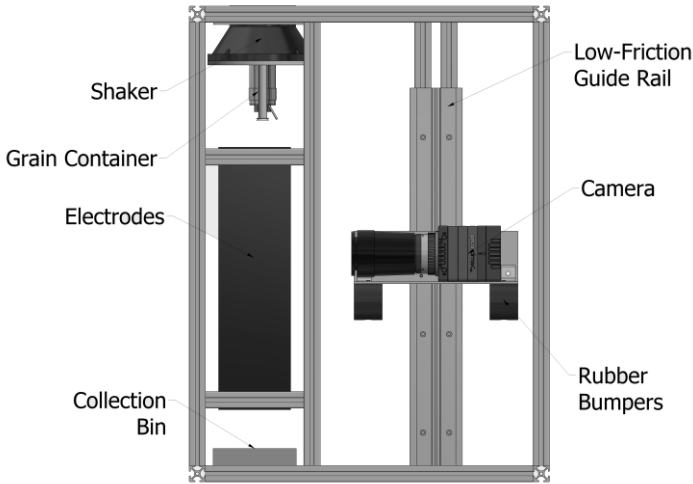
Fig. 1. Experimental apparatus for grain charge measurement. Grains are mixed in the container and dropped through the transverse electric field between the electrodes. The high-speed camera falls alongside the grains and films the acceleration of the grains under the influence of the electric field. The rubber bumpers reduce the impact deceleration to within tolerable limits for the camera.

After a predetermined time (ranging from 1-60 minutes), the mixing is halted and the container releases a small sample of grains. This is performed by triggering an electric motor adjacent to the grain container, which actuates a rotating door on the bottom of the container, as shown in Fig. 2. The door covers a small aperture (diameter $D = 15\ d_{avg}$) in the container. The diameter of this aperture is chosen to prevent granular arching (occurring at < 4-$5\ d_{avg}$ [29-33]) while avoiding clumping in the stream of falling grains (at approximately 19-40 d_{avg} [34-37]). The stream of charged grains falls through the center of the region between the electrodes, so that each grain is subjected to a lateral electric force F_E. As the grains are released, the electromagnet holding the camera carriage is also released, and the camera begins recording, so that the camera falls alongside the grains and films their trajectory. Because the entire device is in high vacuum, neither the grains nor the camera experience appreciable air resistance on their descent, and thus they fall at approximately the same rate. Lights mounted on the camera carriage make the grains more visible against the vertical black backdrop on the other side of the electrodes. When the camera reaches the bottom, it is returned to the top by means of a motorized winch, where the electromagnet re-engages to hold it in place. From here, additional videos can be collected to better characterize the charge distribution.
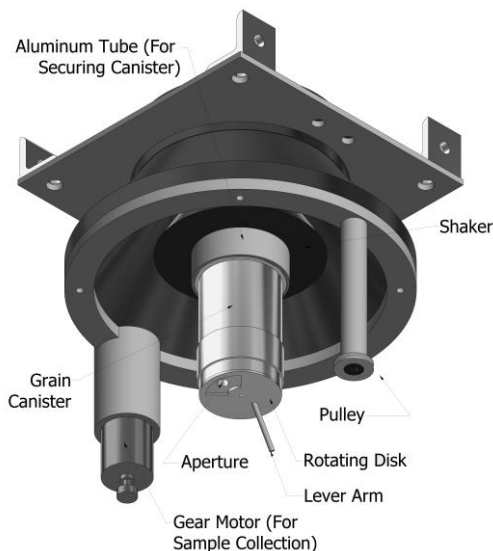
Fig. 2. Grain container and sampling mechanism. A string (not shown) wraps around the motor shaft and pulley, and is attached at a single point to the lever arm. Rotating the motor operates the rotating disk, which toggles the aperture between open and closed. The motor and pulley are not shaken during the mixing process, and the use of a flexible string to connect them to the grain container prevents the shaking process from damaging or dislodging the control mechanism.

III.   DATA PROCESSING

A.   Grain Identification

The experimental apparatus is almost complete. Sample images taken with a different camera were used to verify the performance of the grain identification and tracking algorithm. Fig. 3 displays some sample trajectories taken from these test images. Note that the camera used to collect these images operates at a lower frame rate, exposure time, and overall resolution than the PCO Dimax CS3 we will be using for actual data collection; this is merely for verification of the tracking algorithm. In addition, these images were collected using a stationary camera (relative to the falling grains), and no external electric field was applied to the grains. This resulted in elongation of the grains (due to "motion blur") as seen in the images. This will not be an issue in the final experiment due to the higher frame rate and the fact that the grains and camera will be falling in the same accelerating frame of reference, and will therefore not significantly impact the grain size estimation procedure.
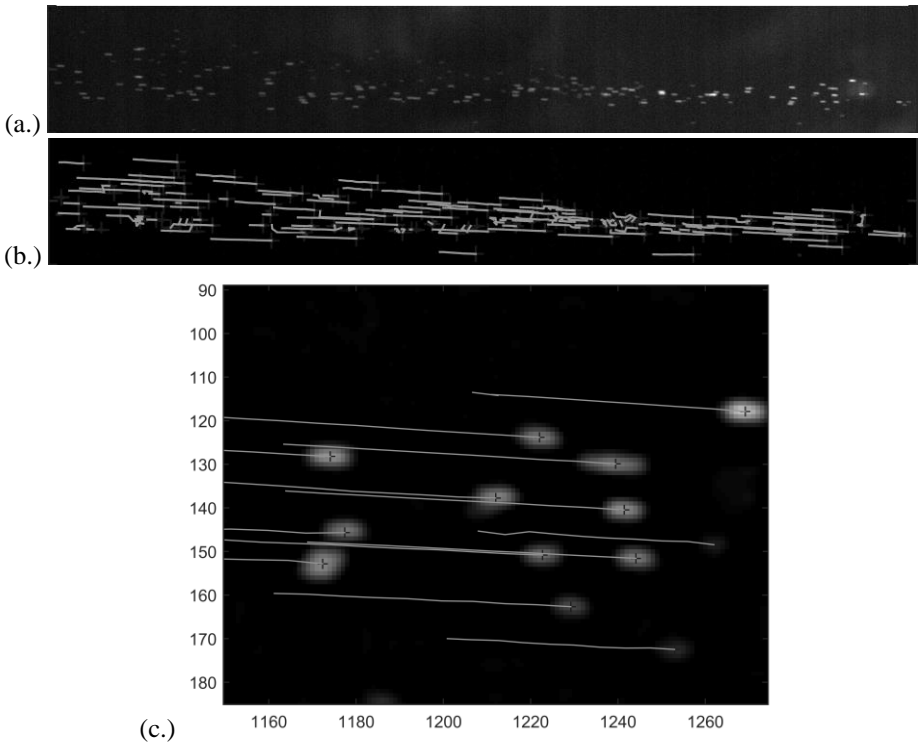
Fig. 3. Sample images for verifying tracking code. (a.) First frame in video, converted to grayscale. (b.) Same image as in (a.), with high-pass filter applied and grain track visualization added. Grain centroids (crosses) and future positions (lines) extracted from later frames are overlaid. Note that the grains are moving from right to left in these images. (c.) Subset of image in (b.) to provide close-up context. Note the jagged trajectory of the faintest grain (bottom right); the low brightness of this grain creates significant errors in centroid determination, leading to tracking errors.

The tracking code utilizes, at its core, a particle tracking algorithm based on an IDL routine developed by Crocker and Grier [38-39], and adapted for implementation in MATLAB [39-40]. We have made substantial modifications to the algorithm, particularly by introducing additional constraints on grain matching to improve match accuracy between frames. In this procedure, frames from the video are first read into the workspace and converted to simple grayscale bitmaps. Then, a high-pass filter is applied to each frame, with the threshold brightness chosen to be approximately equal to the brightness at the edge of each grain. This smooths out the empty background and increases the contrast at the boundary of the grains. Next, the algorithm identifies all local brightness maxima, determines the boundary of the bright region surrounding these points, and calculates the centroid of each region; this represents the physical center of each grain in the image. From here, the algorithm calculates the cross-sectional area of each grain as seen in the image, and estimates its average spherical diameter d_{pix} in pixels. This list of grain centers and sizes is then collected and stored for each frame.

This algorithm will only identify grains whose brightness exceeds the threshold of the

high-pass filter and have well-defined boundaries, so when grains are sufficiently far from the focal plane or are clustered or overlapping, errors can arise. In such a case, the algorithm simply rejects the grain. Clustered grains will not provide meaningful charging data, and the increased errors associated with out-of-focus grains are problematic. Fig. 3c illustrates the effect of low visibility of a grain on its position resolution.

B. Trajectory Determination

As in the experiment performed by Jaeger, *et al*, a taut vertical string passing directly in front of the electrodes, between the camera and the grains, serves as a stable reference point relative to which the images can be calibrated [22]. As the camera falls along the track, it experiences slight perturbations in attitude. By shifting and rotating the images such that the string remains in the same position across all images, we ensure that these small errors are eliminated.

Once the images are properly aligned, the collection of video frames is passed through a matching algorithm. The lists of grain positions are compared for each adjacent pair of frames, and grains between the frames are paired off according to the least-mean-square configuration. For each grain in the first image, a list of possible matches in the second image is compiled. To be considered as a possible match, a grain must be within a predetermined distance Δr from the center of the first grain, where Δr is a parameter equal to the maximum expected distance traveled between frames. In addition, the grain must have an average diameter d_2 within a factor $\Delta d/d_1$ of the first grain's diameter d_1. Finally, because the only forces acting on the grains are gravitational and electrostatic, and the comoving frame of the camera eliminates the effect of gravitational acceleration, we also require that candidate grain pairs have their centers at an angle of no more than θ_{crit} from the horizontal.

Grain trajectories are then compiled by connecting grain pairings across all frames in the video. The tracking algorithm can construct a trajectory even if multiple frames are missing. At this point, any trajectories exhibiting unusual behavior (intersection of two trajectories, collision and subsequent deflection of grains, etc) are flagged and manually inspected, and trajectories that cannot provide sufficient acceleration data are discarded.

C. Charge Calculation

The trajectories found by the tracking algorithm can be used to determine the measured charge and mass of each grain. Each track consists of a set of N horizontal and vertical positions r at times t, as well as a diameter d_{pix} measured at each position (in pixels). Comparing these values with the known density ρ of the grain material (for $SiO_2:ZiO_2$, $\rho = 3800$ kg/m^3) and the known width w of a pixel (based on calibration images taken with a ruler), we can determine the mass of the grain to be:

$$m = \frac{4\pi\rho}{3}\left(\frac{w\sum_N d_{pix}}{2N}\right)^3 \qquad (1)$$

To determine the grain charge, we fit the track's horizontal positions and times to a parabolic trajectory, noting the second-order fit coefficient a_{fit}. This value can be associ-

ated with the particle's acceleration by the following simple relation:

$$\ddot{x} = 2a_{fit} \tag{2}$$

The horizontal acceleration is due solely to the electrostatic force F_E exerted on the particle, which is a function of the grain's mass m and charge q, as well as the electric field strength $E = V/L$, as determined from the applied voltage V and electrode spacing L. The Lorentz force on the particle is therefore given by:

$$F_E = m\ddot{x} = qE \tag{3}$$

The grain charge q can then be given by:

$$q = \frac{2mLa_{fit}}{V} \tag{4}$$

A single video does not contain enough trajectories to sufficiently characterize the charge distribution in a mixture, so we will collect multiple (at least 20) videos for each mixture. Our original model for predicting charge separation related the charge distribution to the size distribution of the mixture, so characterizing the size distribution is also necessary to understand the charge transfer mechanism. We can do this by simply observing a sample of the mixture under a microscope. The measurement in Fig. 4 was taken with the Keyence Digital Microscope at NASA Kennedy Space Center's Electrostatics and Surface Physics Laboratory (ESPL), which automatically filters the image to identify spherical shapes and outputs the size distribution. This provides an accurate size distribution measurement.
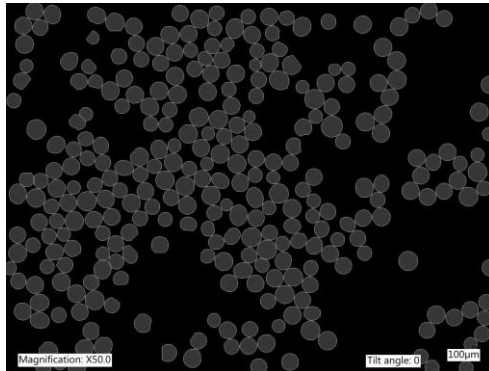
Fig. 4. Outline of silica grains viewed under 50x magnification. The microscope scans the bed of grains, identifies individual grains, filters out aspherical shapes, and estimates the size of the remainder. This method will be used to characterize the size distributions of the granular mixtures used in our experiments.

IV. FUTURE WORK

While our initial plan is to use the described apparatus to test our grain charging predictions [21], we also plan to develop this apparatus to sort granular materials via triboelectric charging. In remote environments like the Moon, Mars, and small airless asteroids, *in situ* resource utilization (ISRU) promises to increase mission length, reliability, and capability by acquiring resources like fuel and building materials from the surrounding environment [41-44]. In particular, using local regolith (surface dust) to create fuels, structures, replacement parts, or other materials is the subject of recent interest [41-44] and will require a process to extract specific size fractions and/or materials from regolith in an efficient manner. We will investigate the viability of material 'sieving' via triboelectric charge exchange once our theoretical charging model has been validated, thus allowing us to predict the charging expected.

V. CONCLUSION

The experimental apparatus we have constructed expands on prior experiments on dielectric grain charging. The falling camera configuration allows us to make precise measurements of individual grain charge and size, and housing the entire device in vacuum allows for greater accuracy at a wider variety of atmospheric conditions. Due to complications associated with inducing tribocharging in air or other ambient gases [14, 24-28], there is a distinct lack of data on the charge distribution in granular mixtures in airless environments like the Moon. We have previously developed a theoretical framework for predicting charge exchange in such environments [21], and this experiment is our next step toward verifying the theoretical model. The flexibility of the experimental procedure also enables us to take steps toward understanding the exact effect of adsorbed water on the charge exchange process. Because we can precisely measure the charge of individual grains using this technique, and therefore get an accurate measurement of the overall charge distribution, it may be possible to identify a charging model that fits both the resulting distribution and the physical collision and charge carrier transfer mechanism. This will significantly improve our understanding of the phenomenon of grain charging in atmosphere. We hope that this will clarify the discrepancies observed between theoretical charging models and experimental evidence.

VI. ACKNOWLEDGMENTS

REFERENCES

[1] T. Pahtz, H. Herrmann, and T. Shinbrot, "Why do particle clouds generate electric charges?" *Nature Physics*, vol. 6, pp. 364-368, May 2010.

[2] J. Kok and N. Renno, "Electrostatics in wind-blown sand," *Physical Review Letters*, vol. 100, Jan 2008.

[3] X. Zheng, N. Huang, and Y. Zhou, "Laboratory measurement of electrification of wind-blown sands and simulation of its effect on sand saltation movement," *Journal of Geophysical Research – Atmospheres*, vol. 108, May 2003.

[4] J. Gilbert, S. Lane, R. Sparks, and T. Koyaguchi, "Charge measurements on particle fallout from a volcanic plume," *Nature*, vol. 349, pp. 598-600, Feb 1991.

[5] I. M. P. Houghton, K. L. Aplin, and K. A. Nicoll, "Triboelectric charging of volcanic ash from the 2011 Grimsvotn eruption," *Physical Review Letters*, vol. 111, no. 118501, Sep. 2013.

[6] K. M. Forward, D. J. Lacks, and R. M. Sankaran, "Triboelectric charging of lunar regolith simulant," *Journal of Geophysical Research*, vol. 114, no. A10109, Oct 2009.

[7] K. M. Forward, D. J. Lacks, and R. M. Sankaran, "Particle-size dependent bipolar charging of Martian regolith simulant," *Geophysical Research Letters*, vol. 36, no. L13201, Jul 2009.

[8] Z. Sternovsky and S. Robertson, "Contact charging of lunar and Martian dust simulants," *Journal of Geophysical Research*, vol. 107, no. E11, Nov. 2002.

[9] S. Trigwell, J. G. Captain, E. E. Arens, J. W. Quinn, and C. I. Calle, "The use of tribocharging in the electrostatic beneficiation of lunar simulant," *IEEE Transactions on Industry Applications*, vol. 45, no. 3, May 2009.

[10] P. Lee, "Dust levitation on asteroids," *Icarus*, vol. 124, pp. 181-194, Nov. 1996.

[11] T. Jackson, W. Farrell, and R. Killen, "Discharging of roving objects in the lunar polar regions," *Journal of Spacecraft and Rockets*, vol. 48, Jul. 2011.

[12] S. Liang, J. Zhang, and L. Fan, "Electrostatic characteristics of hydrated lime powder during transport," *Industrial & Engineering Chemistry Research*, vol. 35, pp. 2748-2755, Aug. 1996.

[13] G. Hendrickson, "Electrostatics and gas-phase fluidized bed polymerization reactor wall sheeting," *Chemical Engineering Science*, vol. 61, pp. 1041-1064, Feb 2006.

[14] P. Cartwright, S. Singh, A. G. Bailey, and L. J. Rose, "Electrostatic charging characteristics of polyethylene powder during pneumatic conveying," *IEEE Transactions on Industry Applications*, 1985.

[15] K. M. Forward, D. J. Lacks, and R. M. Sankaran, "Charge segregation depends on particle size in triboelectrically charged granular materials," *Physical Review Letters*, vol. 102, no. 028001, Jan 2009.

[16] K. M. Forward, D. J. Lacks, and R. M. Sankaran, "Methodology for studying particle-particle triboelectrification in granular materials," *Journal of Electrostatics*, vol. 67, pp. 178-183, May 2009.

[17] H. Zhao, G. S. P. Castle, and I. I. Inculet, "The measurement of bipolar charge in polydisperse powders using a vertical array of Faraday pail sensors," *Journal of Electrostatics*, vol. 55, pp. 261-278, Sep. 2002.

[18] H. Zhao, G. S. P. Castle, I. I. Inculet, and A. G. Bailey, "Bipolar charging of poly-disperse polymer powders in fluidized beds," *IEEE Transactions on Industry Applications*, vol. 39, no. 3, May 2003.

[19] A. Mehrotra, F.J. Muzzio, and T. Shinbrot, "Spontaneous separation of charged grains," *Physical Review Letters*, vol. 99, no. 058001, Jul. 2007.

[20] K. R. Lamarche, X. Liu, S.K. Shah, T. Shinbrot, and B.J. Glasser, "Electrostatic charging during the flow of grains from a cylinder," *Powder Technology*, vol. 195, pp. 158-165, Oct. 2009.

[21] D. Carter and C. Hartzell, "Extension of discrete tribocharging models to continuous size distributions," *Physical Review E*, vol. 95, no. 012901, Jan. 2017.

[22] S. R. Waitukaitis and H. M. Jaeger, "In situ granular charge measurement by free-fall videography," *Review of Scientific Instruments*, vol. 84, no. 025104, Feb 2013.

[23] S. R. Waitukaitis, V. Lee, J. M. Pierson, S. L. Forman, and H. M. Jaeger, "Size-dependent same-material tribocharging in insulating grains," *Physical Review Letters*, vol. 112, no. 218001, May 2014.

[24] S. Pence, V. Novotny, and A. Diaz, "Effect of surface moisture on contact charge of polymers containing ions," *Langmuir*, vol. 10, pp. 592-596, Feb 1994.

[25] A. Wiles, M. Fialkowski, M. Radowski, G. M. Whitesides, and B. Gryzbowski, "Effects of surface modification and moisture on the rates of charge transfer between metals and organic materials," *Journal of Physical Chemsity B*, vol. 108, pp. 20296-20302, Dec 2004.

[26] L. S. McCarty and G. M. Whitesides, "Electrostatic charging due to separation of ions at interfaces: contact electrification of ionic electrets," *Angewandte Chemie International Edition*, vol. 47, pp. 2188-2207, Mar 2008.

[27] Y. Zhang, T. Pahtz, Y. Liu, X. Wang, R. Zhang, Y. Shen, R. Ji, and B. Cai, "Electric field and humidity trigger contact electrification," *Physical Review X*, vol. 5, Jan. 2015.

[28] T. Shinbrot, T. Komatsu, and Q. Zhao, "Spontaneous tribocharging of similar materials," *Europhysics Letters*, vol. 83, Jul 2008.

[29] W. A. Beverloo, H. A. Leniger, and J. van de Velde, "The flow of granular solids through orifices," *Chemical Engineering Science*, vol. 15, no. 3-4, pp. 260-269, Sep. 1961.

[30] K. To, P. Lai, and H. K. Pak, "Jamming of granular flow in a two-dimensional hopper," *Physical Review Letters*, vol. 86, no. 71, Jan. 2001.

[31] K. To, P. Lai, and H. K. Pak, "Flow and jam of granular particles in a two-dimensional hopper," *Physica A*, vol. 315, pp. 174-180, Nov. 2002.

[32] C. Mankoc, A. Janda, R. Arevalo, J. M. Pastor, I. Zuriguel, A. Garcimartin, and D. Maza, "The flow rate of granular materials through an orifice," *Granular Matter*, vol. 9, no. 6, pp. 407-414, Sep. 2007.

[33] C. C. Thomas and D. J. Durian, "Fraction of clogging configurations sampled by granular hopper flow," *Physical Review Letters*, vol. 114, no. 178001, Apr. 2015.

[34] M. E. Mobius, "Clustering instability in a freely falling granular jet," *Physical Review E*, vol. 74, no. 051304, Nov. 2006.

[35] J. R. Royer, D. J. Evans, L. Oyarte, Q. Guo, E. Kapit, M. E. Mobius, S. R. Waitukaitis, and H. M. Jaeger, "High-speed tracking of rupture and clustering in freely falling granular streams," *Nature*, vol. 459, pp. 1110-1113, Jun. 2009.

[36] S. Waitukaitis, H. F. Grutjen, J. R. Royer, and H. M. Jaeger, "Droplet and cluster formation in freely falling granular streams," *Physical Review E*, vol. 83, no. 051302, May 2011.

[37] S. Ulrich and A. Zippelius, "Stability of freely falling granular streams," *Physical Review Letters,* vol. 109, no. 166001, Oct. 2012.

[38] J. C. Crocker and D. G. Grier, "Methods of digital video microscopy for colloidal studies," *Journal of Colloid and Interface Science*, vol. 179, no. 1, pp. 298-310, Apr. 1996.

[39] J. C. Crocker and E. R. Weeks. *Particle Tracking using IDL*. [Online]. Available: http://www.physics.emory.edu/faculty/weeks//idl/

[40] D. Blair and E. Dufresne. *The Matlab Particle Tracking Code Repository*. [Online]. Available: http://site.physics.georgetown.edu/matlab/

[41] C. C. Allen, J. C. Graf, and D. S. McKay, "Sintering bricks on the moon," in *Engineering, Construction, and Operations in Space IV*. Reston, VA: American Society of Civil Engineering, 1994, pp. 1220-1229.

[42] S. Trigwell, J. Captain, K. Weis, and J. Quinn, "Electrostatic beneficiation of lunar regolith: applications in in situ resource utilization," *Journal of Aerospace Engineering*, vol. 26, no. 1, Jan. 2013.

[43] A. Goulas, J. G. P. Binner, R. A. Harris, and R. J. Friel, "Assessing extraterrestrial regolith material simulants for in-situ resource utilization based 3D printing," *Applied Materials Today*, vol. 6, pp. 54-61, Mar. 2017.

[44] J. Carpenter, R. Fisackerly, and B. Houdou, "Establishing lunar resource viability," *Space Policy*, vol. 37, pp. 52-57, Aug. 2016